

UV–Vis spectroscopic and chemometric study on the aggregation of ionic dyes in water

L. Antonov^{a,*}, G. Gergov^b, V. Petrov^c, M. Kubista^d, J. Nygren^d

^a Department of Ecology, National Forestry University, Sofia 1756, Bulgaria

^b Faculty of Pharmacy, Medical University, Sofia 1000, Bulgaria

^c Institute of Organic Chemistry, Bulgarian Academy of Science, Sofia 1113, Bulgaria

^d Department of Biochemistry and Biophysics, Chalmers university of technology, SE-413 90 Gothenburg, Sweden

Received 8 July 1998; received in revised form 3 November 1998; accepted 10 November 1998

Abstract

The monomer–dimer equilibrium in several ionic dyes (Methylene Blue, Acridine Orange, Nile Blue A, Neutral Red, Rhodamine 6G and Safranin O) has been investigated by means of UV–Vis spectroscopy. The data have been processed by a recently developed method for quantitative analysis of undefined mixtures, based on simultaneous resolution of the overlapping bands in the whole set of absorption spectra. In the cases of Acridine Orange a second chemometric approach has been used as a reference. It is based on a decomposition of the recorded spectra into a product of target and projection matrices using non iterative partial least squares (NIPALS). The matrices are then rotated to give the correct concentrations, spectral profiles of the components and the equilibrium constant. The dimeric constants determined by the two methods were in excellent agreement, evidencing the accuracy of the analysis. From the calculated dimeric constant and monomer and dimer spectra, the structures of the dimeric forms of the studied dyes are estimated. © 1999 Elsevier Science B.V. All rights reserved.

Keywords: Aggregation; Chemometrics; UV–Vis spectroscopy; Ionic dyes

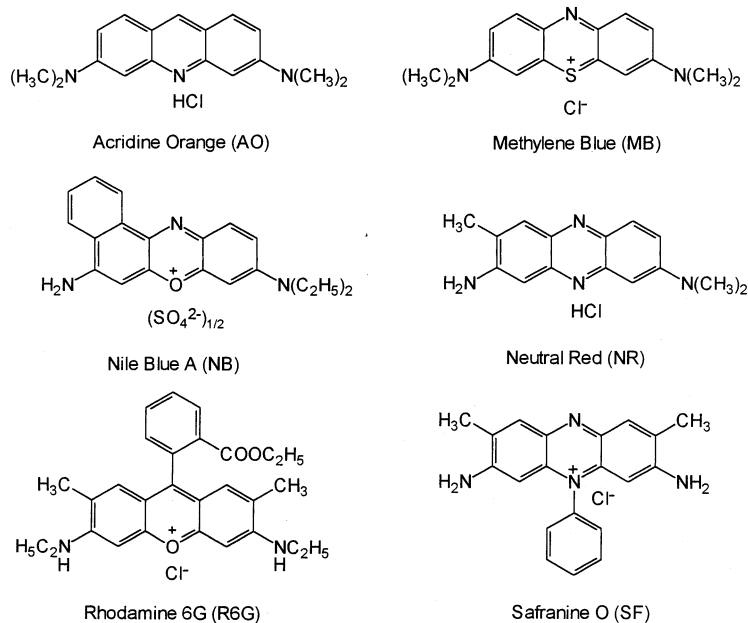
1. Introduction

Aggregation is one of the features of dyes in solution [1–7], affecting their colouristic and photophysical properties and therefore being of special interest. It is well known that the ionic dyes [8,9] tend to aggregate in diluted solutions, lead-

ing to dimer formation, and sometimes even higher order aggregates. In such a case the molecular nature of dye is strongly affected by, and therefore related to such parameters as dye concentration and structure, ionic strength, temperature and presence of organic solvents [10]. Although dyes are very individualistic as structure and, of course behaviour, certain broad rules are well established regarding the aggregation in general. It may increase with an increase of dye concentration or ionic strength; it will decrease

* Corresponding author. Tel.: + 359-2-91907; fax: + 359-2-622830.

E-mail address: lantonov@l.acad.bg; <http://www.orgchm.bas.bg/~lantonov> (L. Antonov)



Scheme 1.

with temperature rising or organic solvents adding; addition to the dye structure of ionic solubilizing groups (as sulphonate group) will decrease aggregation, whereas the inclusion of long alkyl chains [11] increases aggregation because of higher hydrophobic interaction in solution.

The absorption UV–Vis spectroscopy is one of the most suitable methods for quantitative studying the aggregation properties of dyes as function of concentration, since in the concentration range used (10^{-3} – 10^{-6} M) mainly monomer-dimer equilibrium exists.



There are numerous UV–Vis spectroscopy studies on the aggregation, but surprisingly their results are frequently inconsistent and sometimes contradictory [10,12], particularly for studies carried out on the same dye. For example the value of dimeric constant of Methylene Blue varies from 1500 to 55 600 or in orders [12]. This unsatisfactory situation arises from two main reasons, ill defined experimental conditions (the purified or commercial dye is used) and numerous assumptions made in the processing of the spectral data

[2,3,13–17]. The latter is a consequence of that the individual spectra of the components (monomer and dimer) cannot be measured experimentally, which renders classical spectrophotometry impossible.

Therefore the aim of the present paper is to apply the recently developed approach for quantitative analysis [18] to study the monomer–dimer equilibrium in the case of several wide used ionic dyes (Scheme 1) and to confirm the results by processing the same data by an independent chemometric approach based on matrix calculations [19].

2. Experimental part

The investigated dyes (for microscopy grade) were purchased from Fluka and Aldrich and were studied without additional purification (except SF). The experiment was carried out in distilled water, keeping the cell thickness (l) and total dye concentration (c^*) so that $l \cdot c^* = \text{constant}$. The absorption spectra were measured on a PE Lambda 5 UV–Vis spectrophotometer. The data

for each dye were stored in spectral files as matrices of size m (wavelengths) and p (concentrations) and then processed by using MULTIRES [18] and DATAN [19,20] packages.

3. Theoretical part

The analysis of monomer–dimer equilibria consists of two consecutive steps: (i) estimation of the dimeric constant (which provides information about aggregation-dye structure relation); and (ii) studying the dimer structure (which depends on the electronic interaction between the two dye molecules in the dimer).

3.1. Estimation of the dimeric constant

The basic relations describing a monomer (M)–dimer (D) equilibrium as a function of the dye concentration are:

Beer's law:

$$A_{i,j}^* = \varepsilon_j^M \cdot c_i^M \cdot l_i + \varepsilon_j^D \cdot c_i^D \cdot l_i = A_j^M \cdot x_i^M + A_j^D \cdot x_i^D, \quad (1)$$

Mass balance:

$$c_i^M + 2c_i^D = c_i^* \quad (2)$$

$$\text{or, } x_i^M + x_i^D = 1 \quad (3)$$

Dimeric constant:

$$K_D = \frac{c_i^D}{(c_i^M)^2} = \frac{x_i^D}{2c_i^* (x_i^M)^2} \quad (4)$$

where: i ($i = 1 - p$) and j ($j = 1 - m$) denote i^{th} concentration and j^{th} wavelength, A^* is the measured absorbance, ε^M and ε^D are the molar absorptivities of monomer and dimer, respectively, c^M and c^D are the concentrations of monomer and dimer, respectively.

The molar fractions (x) and partial absorbances (A) are defined according to Eqs. (5)–(8):

$$x_i^M = \frac{c_i^M}{c_i^*} \quad (5)$$

$$x_i^D = \frac{2c_i^D}{c_i^*} \quad (6)$$

$$A_j^M = \varepsilon_j^M \cdot c_i^* \cdot l_i \quad (7)$$

$$A_j^D = \frac{\varepsilon_j^D}{2} \cdot c_i^* \cdot l_i \quad (8)$$

If the individual spectra of M and D are known it would be easy to calculate the molar fractions and dimeric constant. However the individual spectrum of the dimer cannot be obtained experimentally because the increase of c^* causes formation of higher order aggregates. Further, the spectrum of the monomer could in principle be measured in a highly diluted solution, but such a spectrum is often very noisy leading to considerable uncertainty in the analysis [3]. For these reasons the quantitative analysis of monomer–dimer equilibria represents a case of analysis of undefined mixtures, which cannot be solved by the methods of classical spectrophotometry.

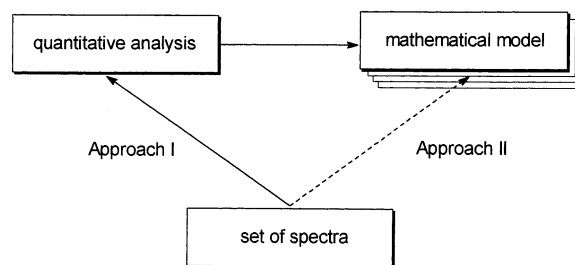
The two possible ways for analysis of such mixtures without a priori assumptions are shown in Scheme 2. The first one is directed primary to quantitative analysis (i.e. calculation of the molar fractions and then the individual spectra) without any model assumptions of the system investigated. That could be done using:

- additional spectral information as finding individual areas of absorbance,
- resolution of overlapping bands [18,21,22],
- derivative spectroscopy [23].

After performing the quantitative analysis, the molar fractions are used for adopting a suitable model (from several existing) of the system.

The second approach starts by choosing a mathematical model and, using the experimental data, fitting the spectral responses [19,20,24,25].

Both approaches have their advantages and disadvantages, but (and most important) if no assumptions have been made when fitting Eq. (1),



Scheme 2.

the results of the approaches should be identical in the frame of some computational errors.

In the present study the two methods were used to treat the same data to allow stringent comparison.

3.1.1. Method 1

It is well known that each UV–Vis absorption spectrum could be presented as superposition of Gauss functions (F) describing its individual bands [26,27]. In such a case the individual spectra of M and D can be expressed as:

$$A_j^M = \sum_{k=1}^{n_M} F(\lambda_j, A_{\max_k}^M, \lambda_{\max_k}^M, \Delta v_{1/2_k}^M) \quad (9)$$

$$A_j^D = \sum_{s=1}^{n_D} F(\lambda_j, A_{\max_s}^D, \lambda_{\max_s}^D, \Delta v_{1/2_s}^D) \quad (10)$$

where n_M and n_D are numbers of individual bands composing the individual spectrum of M and D, respectively ($n_M + n_D = n$), A_{\max} , λ_{\max} , $\Delta v_{1/2}$ are the three basic spectral parameters (intensity, position and band width) describing the definite individual band.

According to Eqs. (3), (9) and (10) the Eq. (1) can be written as follows:

$$A_{i,j} = x_i^M \cdot \left\{ \sum_{k=1}^{n_M} F(\lambda_j, A_{\max_k}^M, \lambda_{\max_k}^M, \Delta v_{1/2_k}^M) - \sum_{s=1}^{n_D} F(\lambda_j, A_{\max_s}^D, \lambda_{\max_s}^D, \Delta v_{1/2_s}^D) \right\} + \sum_{s=1}^{n_D} F(\lambda_j, A_{\max_s}^D, \lambda_{\max_s}^D, \Delta v_{1/2_s}^D) \quad (11)$$

Eq. (11) correctly (from both mathematical and physical point of view) describes the real measured spectrum and allows an optimisation function, characterised by $3n + p$ optimisation parameters ($3n$ basic parameters for the individual bands and p unknown monomer molar fractions) and pm experimental points, to be defined:

$$S_1^2 = \frac{\sum_{i=1}^p \sum_{j=1}^m (A_{i,j}^* - A_{i,j})^2}{p \cdot m} \quad (12)$$

where A^* is the measured absorbance, while A is the calculated one according to Eq. (11).

The values of the individual bands basic parameters (and the individual spectra of M and D according to Eqs. (9) and (10)) and monomer molar fractions in each solution can be obtained after minimization of Eq. (12) using two step optimization procedure [18]. Note that the minimization procedure, which is implemented in the program MULTIRES [18], is valid for any two components mixture; that the components are involved in a monomer–dimer equilibrium is not used as criterion (i.e. no model assumptions are made).

Then the molar fractions obtained could be plotted versus c^* in the linear equation (where log denotes base 10 logarithm):

$$\log c_i^* = \log \frac{1 - x_i^M}{2(x_i^M)^2} - \log K_D \quad (13)$$

which results from Eqs. (4) and (3).

The slope of the curve, which has to tend to 1, is used as a criterion of adopting monomer–dimer model.

3.1.2. Method 2

A chemometric approach for quantitative analysis, based on decomposition of the matrix A^* into a product of target and projection matrices [19] was used for comparison. Its application for analysis of monomer–dimer equilibria has been described in details previously and the approach is implemented in the program DATAN [19]. DATAN uses matrix A^* and calculates the value of K_D (optimised stepwise), the individual spectra and molar fractions of both species.

As a fitting function the Eq. (14) is used:

$$S_2^2 = \frac{\sum_{i=1}^p \sum_{j=1}^m \left(A_{i,j}^* - \frac{\sqrt{1 + 8c_i^* \cdot K_D} - 1}{4c_i^* \cdot K_D} \cdot (A_j^M - A_j^D) - A_j^D \right)^2}{p \cdot m} \quad (14)$$

3.2. Estimation of dimer structure

The spectral changes observed upon dimer formation are caused by electronic interactions between the dye molecules in the dimer. Identical

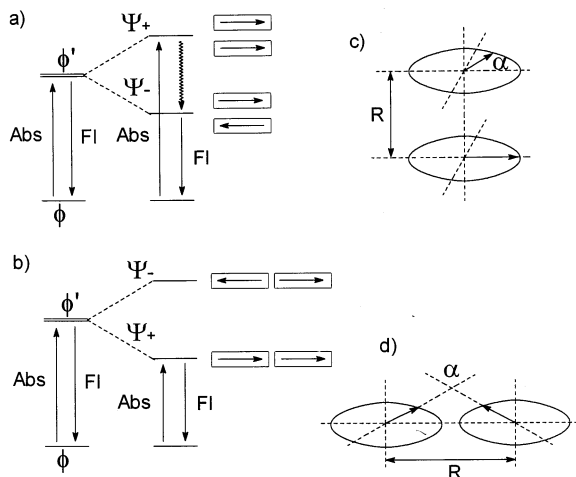


Fig. 1. Energy graphs and structure of 'sandwich' (a and c) and 'head to tail' (b and d) dimers.

dye molecules with ground state wavefunctions ϕ_1 and ϕ_2 and singlet excited state wavefunctions ϕ'_1 and ϕ'_2 , have in dimeric state the ground state wavefunction:

$$\Psi_0 = \phi_1 \cdot \phi_2 \quad (15)$$

In the excited state the dimer wavefunctions are split into symmetric and asymmetric combinations:

$$\Psi_+ = \frac{1}{\sqrt{2}} \cdot (\phi'_1 \cdot \phi_2 + \phi_1 \cdot \phi'_2) \quad (16)$$

$$\Psi_- = \frac{1}{\sqrt{2}} \cdot (\phi'_1 \cdot \phi_2 - \phi_1 \cdot \phi'_2) \quad (17)$$

The energies of these two states are consequently different.

According to the molecular exciton theory [28,29] there are two ideal cases of dimer structure:

1. 'Sandwich' dimer (Fig. 1a)—the transition moments of both monomer molecules are one direction parallel in the higher energy state Ψ_+ , which means that the intensity (and oscillator strength) of the transition $\Psi_0 \rightarrow \Psi_+$ is substantial. The opposite is true for the lower energy transition. As a result in the absorption spectrum of dimer a band (called 'H-band'), shifted hypsochromic in respect of pure monomer one, appears.

2. 'Head to tail' dimer (Fig. 1b). The transition $\Psi_0 \rightarrow \Psi_-$ is forbidden, because of the opposite directions of the transition moments. However the lower energy transition is permitted and a bathochromic band ('J-band') appears in the dimer spectrum.

In general the both cases of the dimer are idealistic and in the reality the transition moments are neither parallel or anti-parallel, which leads to appearance of both H- and J-bands in the dimer spectrum (Fig. 1c, d) with energy difference between them:

$$\Delta v = v_H - v_J \quad (18)$$

Their relative intensities depend on the angle α between the transition moments, which is defined as:

$$\alpha = 2 \arctan \frac{\sqrt{v_H \cdot f_J}}{\sqrt{v_J \cdot f_H}} \quad (19)$$

where v is the position (in cm^{-1}) and f is the oscillator strength of the corresponding transition. The distance (R in Å) between the monomers in the dimer could be find by the expression:

$$R = \sqrt[3]{\frac{2 \cdot 14 \times 10^{10} \cdot \cos \alpha \cdot f_M}{\Delta v \cdot v_M}} \quad (20)$$

where M denotes the oscillator strength and energy of the transition in the pure monomer.

Of course this theoretical model is too simplified description of the interactions in the dimer and the crude physical basis of Eq. (20) has to be taken into account. While comparison of related dyes is rather straight forward, one should interpret the absolute values of R with concern.

4. Results and discussion

The absorption spectra of AO recorded as a function of the dye concentration are shown in Fig. 2a. Increasing total dye concentration leads to a decrease in the intensity of the monomer band at 490 nm and a new maximum at 460 nm appears signifying the formation of dimer.

The set of spectra was analysed by method 1 and the most suitable fit of Eq. (12) ($S_1^2 = 1 \cdot 191 \cdot 10^{-4}$) was obtained when the spectra of M

and D have been described by 6 ($n_M = 6$) and 5 ($n_D = 5$) individual bands respectively. The general calculational conditions of resolution procedure were described previously [18,26,27]. The spectra of both species, reconstructed according to Eqs. (9) and (10) are presented in Fig. 2b. It should be noted especially that the calculated spectrum of the dimer predicts both H- and J-bands according to the theory discussed above. The values of the monomer molar fractions calculated in the optimization procedure are collected in Table 1 as a function of the dye concentration. The plot of Eq. (13) showed good correlation (0.998) with a slope 0.88. The deviation from 1, which is expected for a monomer dimer equilibrium, might result from the experimental noise in the recorded spectra and also from errors in the nonlinear optimization procedure when calculat-

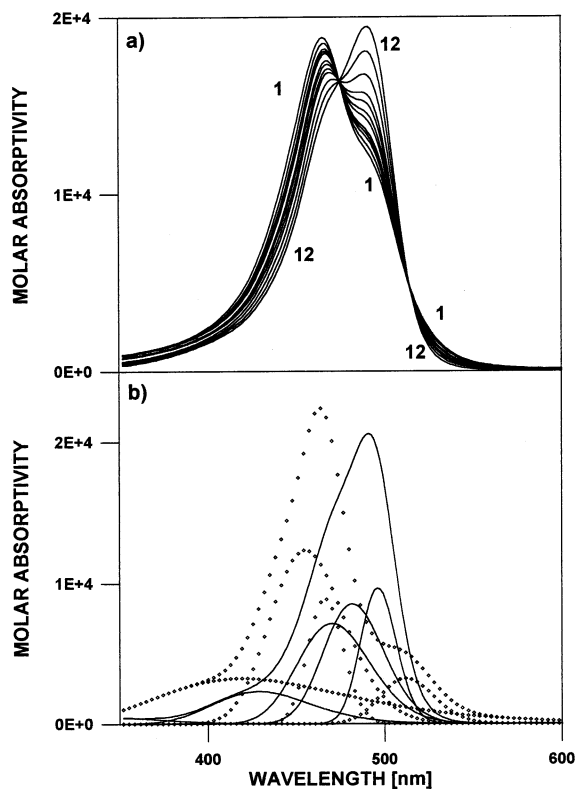


Fig. 2. (a) Absorption spectra of AO in water recorded as different concentrations (see Table 1); (b) calculated individual spectra ε^M (solid line) and $\varepsilon^D/2$ (dots) with their composing individual bands.

Table 1
Calculated molar fractions (%) of the monomer

i	$c_i \cdot 10^4$ (mol l $^{-1}$)	Method 1	Method 2
1	11.01	43.4	43.2
2	7.200	48.0	50.1
3	6.372	51.6	52.1
4	5.740	53.5	53.9
5	5.031	55.2	56.1
6	4.320	61.1	58.7
7	3.600	63.8	61.9
8	2.880	67.9	65.6
9	2.160	71.8	70.4
10	1.440	79.3	76.6
11	0.720	87.3	85.4
12	0.288	95.4	93.1

ing the molar fractions. The values of $\log K_D$ were calculated for each solution using Eq. (4) and the final mean result was estimated as 3.10 ± 0.06 .

The same raw data (Fig. 2a) were processed by method 2 and after stepwise optimization of $\log K_D$ (Fig. 3) the best fit ($S_2^2 = 1.583.10^{-4}$) was found at $\log K_D = 3.14$. The calculated monomer molar ratios are very close to those obtained from the first analysis (Table 1). The calculated monomer and dimer spectra were essentially identical to those from the first analysis depicted in Fig. 2b.

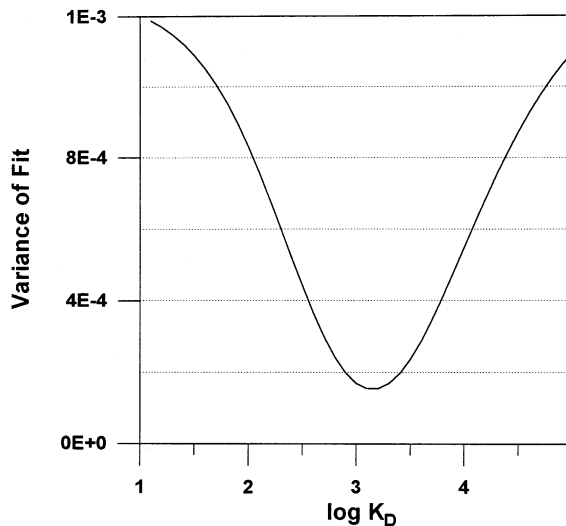


Fig. 3. Stepwise optimization of $\log K_D$ of AO in water.

Table 2
Dimeric constants and structure parameters of the dimer calculated by method 1

	Dye					
	AO	MB	NR	NB	R6G	SF
$\log K_D$	3.10	3.6	3.27	3.09	3.50	4.3
SD	0.06	0.1	0.03	0.05	0.06	0.1
Monomer						
ν_M (cm ⁻¹)	20 370	15 060	18 660	15 750	18 980	19 050
f_M	0.182	0.502	0.268	0.377	0.604	0.431
Dimer						
ν_H (cm ⁻¹)	21 550	16 530	19 800	17 180	20 080	20 160
ν_J (cm ⁻¹)	19 530	14770	17 300	14 680	18 830	19 460
f_H	0.356	1.028	0.764	2.334	1.086	0.583
f_J	0.041	0.159	0.094	0.334	0.074	0.166
$\Delta\nu$ (cm ⁻¹)	2020	1760	2500	2500	1250	700
α (°)	39	45	41	45	30	57
R (Å)	4.2	6.6	4.5	5.3	7.8	7.2

The calculated $\log K_D$ values by the two methods are essentially the same, even though they use quite different approaches. This confirms their reliability and evidences that they both are appropriate for analysing monomer-dimer equilibria.

Knowing the spectra of the monomer and dimer it is possible to make conclusions about the dimer structure. Usually a detailed analysis requires the dimer spectrum to be resolved into the H- and J-bands, but this is not necessary here because these parameters were obtained already in the optimisation procedure (Fig. 2b). The positions, intensities and band widths of the individual bands were determined, which makes it possible to calculate energies and oscillator strengths of the electronic transitions involved [27].

The values for the $\log K_D$ as well as the structural parameters of the corresponding dimers for the investigated ionic dyes, obtained according to the present approach are collected in Table 2. The differences in the calculated structural parameters for the different dyes are rather small, suggesting that they all have similar structures. This is reasonable in view of that they all have a core of three fused aromatic rings, with a central heteroatom. The calculated monomer–monomer distances are 4–8 Å, excluding end-to-end

arrangement. The angles between the dye transition moments are 30–60°, suggesting that the two monomer dyes stack on top of each other, being significantly rotated. The dyes' permanent dipole moment should, for some of them owing to symmetry reasons and for the other owing to the heteroatoms, be directed essentially along the molecular short axis. The dyes should therefore stack in opposite direction (i.e. top to bottom) for the dipoles to interact attractively. The dyes are also expected to be highly polarizable owing to their large aromatic systems, and the polarizability tensor should have the largest component along the molecular long axis. This is probably the reason for the monomers to be twisted, since that may optimize the permanent dipole–induced-dipole interactions.

5. Conclusions

A new approach for analysis of monomer–dimer equilibria, based on the simultaneous resolution of individual bands in a set of spectra, is proposed. It determines the monomer molar ratios in the samples, as well as the monomer and dimer spectra with high accuracy, as evidenced by comparison with the DATAN approach. The re-

sults of the analysis can be used to extract information about electronic interactions of the dye monomers in the dimer, from which the dimer structure can be deduced.

Acknowledgements

The comments of the unknown reviewers is greatly helpful. Financial support from the National Science Found and Eureka Foundation is gratefully acknowledged (LA).

References

- [1] S.E. Cheppard, Proc. R. Soc. 82A (1909) 256.
- [2] A.R. Monahan, D.F. Brossey, J. Phys. Chem. 74 (1970) 1970.
- [3] W. West, S. Pearce, J. Phys. Chem. 69 (1965) 1894.
- [4] K. Bergmann, C. O'Konski, J. Phys. Chem. 69 (1965) 1884.
- [5] W. Stork, G. Lippits, M. Mandel, J. Phys. Chem. 76 (1972) 1772.
- [6] B. Craven, A. Datyner, JSDC 79 (1963) 515.
- [7] A.R. Monahan, J.A. Brado, A.F. Delura, J. Phys. Chem. 76 (1972) 1972, 1994.
- [8] J. Georges, Spectrochim. Acta 51A (1995) 985.
- [9] T. Stoyanova, L. Antonov, D. Dimitrov, S. Stoyanov, Ann. Univ. Sofia 87 (1995) 55 (Bulg.), Chem. Abstr. 125:316864j.
- [10] B.C. Burdett, Aggregation of dyes, in: Studies in Physical and Theoretical Chemistry, vol. 28, Elsevier, 1983, p. 241.
- [11] T. Iijima, E. Jojima, L. Antonov, S. Stoyanov, T. Stoyanova, Dyes Pigm. 37 (1998) 81 (and references cited therein).
- [12] Some results for the dimer constant of Methylene Blue: 1500, A.K. Busenbaev, L.B. Zouaou, A.M. Saletskii, Zh. Prikl. Spekt. 52 (1989) 424; 8900, reference 9; 9600, C. Lee, Y.W. Sung, J.W. Park, Anal. Sci. 13 (1997) 167; 55600, Suzuki, K. Tsuchiya, M. Bull. Chem. Soc. Jpn. 44 (1971) 967.
- [13] K.K. Rohatgi, J. Mol. Struct. 27 (1968) 545.
- [14] J. Lavorel, J. Phys. Chem. 61 (1957) 1000.
- [15] I.L. Arbeloa, J. Chem. Soc. Faraday Trans. 2 (77) (1981) 1725.
- [16] F. Lopez, Y. Liebana, E.C. Fernandez, I.L. Arbeloa, Spectrochim. Acta 45A (1989) 1201.
- [17] S. Stoyanov, T. Deligeorgiev, D. Simov, J. Mol. Struct. 115 (1984) 363.
- [18] L. Antonov, D. Nedeltcheva, Anal. Lett. 29 (1996) 2055.
- [19] M. Kubista, R. Sjoback, B. Albinson, Anal. Chem. 65 (1993) 994.
- [20] I. Scarmino, M. Kubista, Anal. Chem. 65 (1993) 409.
- [21] L. Antonov, S. Stoyanov, Anal. Chim. Acta 314 (1995) 225.
- [22] M.C. Argoni, M. Arca, G. Crisponi, V.M. Nurchi, Anal. Chim. Acta 316 (1995) 195.
- [23] N. Mateeva, L. Antonov, M. Mitewa, S. Miteva, Talanta 43 (1996) 275.
- [24] J.F. Rusling, Crit. Rev. Anal. Chem. 21 (1989) 49.
- [25] F. Peral, J. Mol. Struct. 266 (1992) 373.
- [26] L. Antonov, S. Stoyanov, Appl. Spectrosc. 47 (1993) 1030.
- [27] L. Antonov, Trends Anal. Chem. 16 (1997) 536.
- [28] M. Kasha, H.R. Rawls, M.A. El-Bayomi, Pure Appl. Chem. 11 (1965) 371.
- [29] S.F. Mason, JSDC 84 (1968) 604.